

PARTIAL POWER CONVERTERS IN MOBILE MODULAR ROBOT POWER SUPPLY SYSTEM

Rodions Saltanovs¹, Alexey Shevchenko²

¹Riga Nordic University, Latvia; ²SIA "RS DYNAMICS", Latvia
bk201@inbox.lv, alexey@cryptolab.net

Abstract. This paper investigates the use of a 36 V common DC bus and bidirectional partial-power processing converters in the onboard power supply system of a mobile modular robot. The novelty of the study is the application and experimental validation of a bidirectional partial-power conversion approach for a low-voltage robotic module operating in both traction and regenerative modes. Unlike most previous partial-power converter studies focused on photovoltaic systems, battery interfaces, microgrids, or charging infrastructure, this work considers a mobile robotic power architecture with a common DC bus and compares a partial-power converter with a conventional bidirectional full-power DC-DC converter implemented on the same component base. For the considered module, the traction operating point is 24 V and 22 A, while the regenerative operating point is 16 V and 10 A. The processed-power fraction is analytically estimated and then evaluated experimentally under steady-state operating conditions. Under ideal power-sharing assumptions, the active partial-power stage processes 176 W, or 33.3% of 528 W, in traction mode and 88.9 W, or 55.6% of 160 W, in regenerative mode. The experimental comparison shows that converter losses decrease from 14.35 W to 3.42 W in traction mode and from 4.70 W to 2.74 W in regenerative mode. These results confirm that partial-power conversion is most beneficial when the module voltage remains close to the common-bus voltage and can reduce thermal stress and cooling requirements in modular robotic platforms.

Keywords: robot, PPC, DC bus, converter, regeneration, efficiency.

1. Introduction

For mobile wheeled robots, the energy efficiency of the onboard power supply system is a key factor that directly affects autonomous operating time, cooling-system mass, and allowable payload. Even moderate losses in auxiliary DC-DC converters reduce mission duration and increase the thermal load inside the robot enclosure [1; 2].

In conventional architectures, regulated supply rails are derived from the main battery through full-power converters. In that case, the entire power flow passes through the active conversion stage, so conduction, switching, and magnetic losses scale with the transferred power. Partial power processing (PPC) offers an alternative: only the fraction of power required to match the source and load voltages is processed by the active stage, while the remaining power is delivered through a direct path [3; 4].

Although PPC has been studied extensively in photovoltaic systems, energy storage interfaces, DC microgrids, and charging infrastructure, comparatively few publications address its use at the level of a practical onboard power architecture for mobile robots. In particular, the combination of a low-voltage common DC bus, bidirectional operation, regenerative energy flow, and a controlled comparison with a conventional bidirectional converter on the same hardware platform is still insufficiently documented. Therefore, the novelty of this study is the experimentally validated application of a bidirectional PPC architecture to a representative low-voltage robotic module operating in both traction and regenerative modes. The contribution of this paper is threefold: first, a bus-based power architecture for a mobile modular robot is proposed; second, the processed-power fraction is quantified for representative traction and regeneration operating points; and third, the proposed PPC configuration is experimentally compared with a full-power bidirectional converter implemented using the same component base.

2. Literature Review

The basic idea of PPC is that regulation does not require the converter to process the full load power. This point was illustrated clearly by Agamy et al. [3] and later by Zientarski et al. [4], who also emphasized an important caveat: a reduced processed-power fraction does not automatically guarantee a superior architecture, because internal power circulation and the total stress on the power stage must also be considered.

Subsequent studies developed formal applicability criteria, topology classifications, and fair comparison methods. References [5-7] showed that the benefit of PPC depends on the regulation range, the way the base converter is inserted into the system, and the fraction of power bypassing the active

stage. Review papers [8-10] systematized PPC architectures and terminology, while studies [11-13] linked achievable efficiency to the selected topology and operating regime.

Application-oriented studies [14-17] confirmed that PPC is particularly attractive for battery interfaces, DC microgrids, and charging systems in which source and load voltages are relatively close. However, for distributed onboard power networks in mobile robots, an applied design perspective is still needed: the choice of architecture, the expected processed-power fraction, the behaviour in regenerative operation, and a fair experimental comparison with a conventional full-power converter.

These studies provide an important theoretical and application-oriented basis for the use of PPC in systems where source and load voltages are relatively close. However, most reported applications concern photovoltaic conversion, stationary energy storage, DC microgrids, or charging systems. In contrast, mobile modular robots impose additional constraints, including compactness, limited cooling capability, bidirectional module operation, regenerative energy return, and changing mission-dependent load configurations. Therefore, a direct experimental comparison between PPC and full-power conversion under representative robotic operating conditions is still required.

3. Power-System Architecture of the Mobile Modular Robot

In a modular mobile robot, a centralized power architecture with a single source and a fixed set of loads is often too rigid. In practice, the platform configuration changes with the mission: propulsion modules, energy-storage units, recuperative drives, and local energy sources can be connected to the same system. It is therefore reasonable to treat the onboard power supply as an intelligent energy network built around a common DC bus to which energy-active nodes of different types are connected.

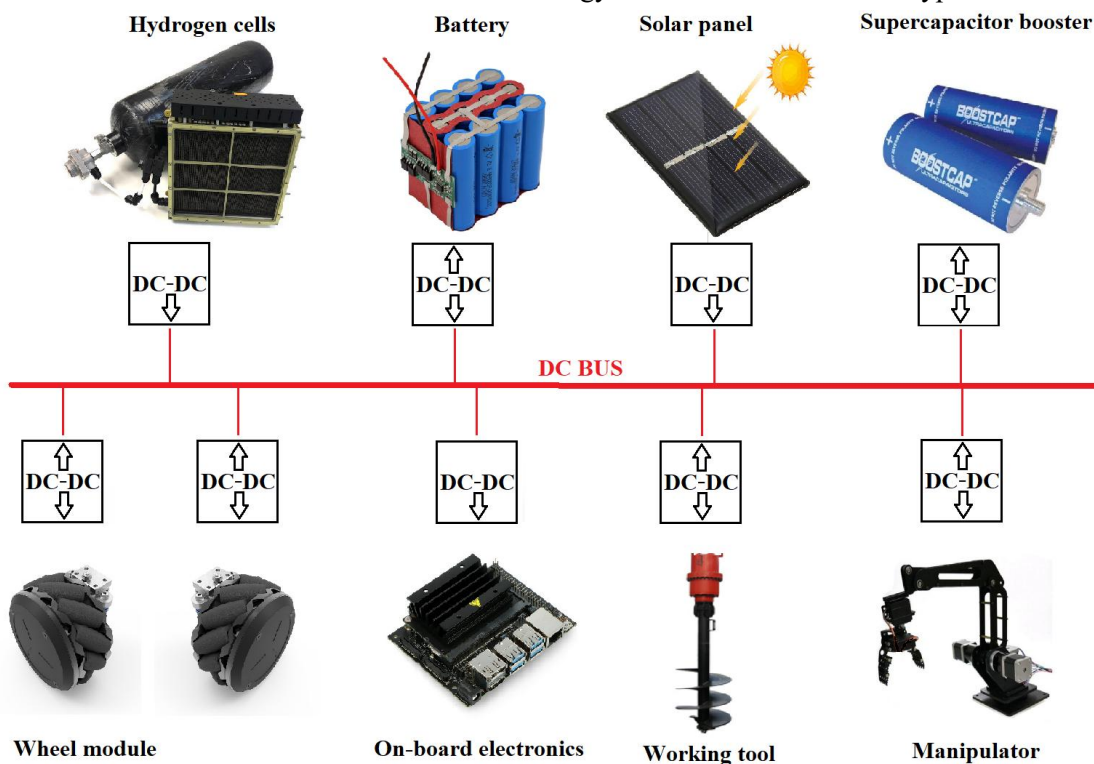


Fig. 1. Conceptual power architecture of the mobile modular robot with a common DC bus

In such an architecture, each module has a power interface and a communication channel to the supervisory power-management controller, for example, via a CAN bus. This makes it possible to exchange information about admissible consumption and generation power, state of charge, operational priority, and allowed operating modes. Based on this information, the energy manager distributes the available power, limits secondary loads when necessary, and coordinates regenerative energy flows.

The main drawback of a distributed modular architecture is the larger number of conversion stages and, consequently, higher cumulative losses. This problem is especially pronounced in systems where energy repeatedly moves between different voltage levels: from the battery to the common bus, from

the bus to an actuator module, and back again during regeneration. For modules which voltage remains relatively close to the bus voltage, PPC is therefore a logical choice because it reduces the amount of energy that must be processed actively and lowers the thermal stress on the power electronics.

4. Bidirectional PPC Converter for a Module with Traction and Regeneration Modes

4.1. Operating Conditions

The considered energy-active module is connected to a common DC bus with voltage $U_b = 36$ V. In traction mode, the module operates at terminal voltage $U_{tr} = 24$ V and maximum current $I_{trMax} = 22$ A. In regenerative mode, the module returns energy at terminal voltage $U_{reg} = 16$ V and maximum current $I_{regMax} = 10$ A. These operating points were selected as representative maximum steady-state conditions for comparing partial-power and full-power bidirectional conversion.

Table 1

Operating conditions of the considered module

Parameter	Symbol	Value
Common-bus voltage	U_b	36 V
Traction-mode module voltage	U_{tr}	24 V
Maximum traction-mode current	I_{trMax}	22 A
Regenerative-mode module voltage	U_{reg}	16 V
Maximum regenerative current	I_{regMax}	10 A

4.2. Estimation of Processed Power

To estimate the architectural benefit of the proposed PPC converter, the processed power was first evaluated under ideal steady-state conditions, neglecting converter losses. Let U_b denote the common-bus voltage, and let U_x and I_x denote the module terminal voltage and current in operating mode x , where $x \in \{tr, reg\}$. The total module power in each mode is defined as

$$P_x = U_x I_x. \quad (1)$$

For the considered series-connected PPC arrangement, only the voltage-mismatch part of the total power is processed by the active converter stage. Therefore, the processed-power fraction can be expressed as

$$k_{proc,x} = \left| 1 - \frac{U_x}{U_b} \right|. \quad (2)$$

The corresponding processed power of the active PPC stage is then

$$P_{proc,x} = k_{proc,x} P_x. \quad (3)$$

Using the operating conditions from Table 1, the traction-mode module power is $P_{tr} = 528$ W. Since $U_{tr} = 24$ V and $U_b = 36$ V, the processed-power fraction is $k_{proc,tr} = 0.333$. Thus, the active PPC stage processes $P_{proc,tr} = 176$ W, which corresponds to 33.3% of the total traction power.

In regenerative mode, the returned module power is $P_{reg} = 160$ W. For $U_{reg} = 16$ V and $U_b = 36$ V, the processed-power fraction is $k_{proc,reg} = 0.556$. Therefore, the active PPC stage processes $P_{proc,reg} = 88.9$ W, which corresponds to 55.6% of the total returned power.

These estimates show that the benefit of the PPC architecture is directionally asymmetric. In traction mode, the module voltage is closer to the common-bus voltage, so only one third of the total power is processed by the active stage. In regenerative mode, the voltage mismatch is larger, which increases the processed-power fraction and reduces the relative advantage of PPC.

4.3. Converter Topology and Operating Modes

Structurally, the converter includes a direct power path that transfers the main share of the energy, a bidirectional active PPC cell based on a synchronous buck-boost function, input and output filters,

voltage/current/temperature sensors, and a controller that provides current limiting, operating-point stabilization, and communication with the central power manager of the robot.

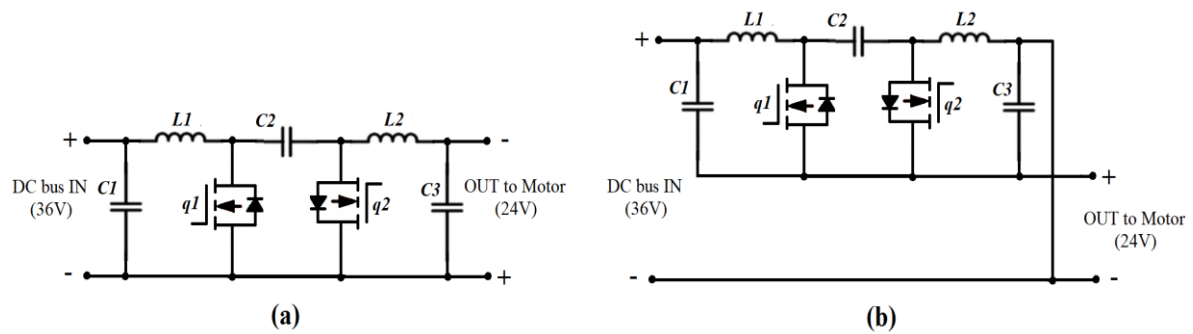


Fig. 2. Bidirectional Cuk converter implemented as (a) a full-power converter and (b) a PPC converter

From the standpoint of system operation, four modes are relevant: (1) traction mode, in which the module is powered from the common bus; (2) regenerative mode, in which energy is returned to the bus; (3) standby mode with minimal self-consumption; and (4) a protective mode that limits regeneration when the common bus cannot absorb the returned energy. The protective mode is essential to prevent bus overvoltage; in a practical system, it requires either a buffer storage element or a controlled dissipation path.

A bidirectional Cuk converter was selected as the hardware basis because it supports bidirectional power flow and allowed the same hardware platform to be configured either as a conventional full-power converter or as a PPC converter with only minor modifications. The switching frequency was set to 50 kHz, consistent with the capabilities of the selected hardware.

The prototype was implemented using an STM32F103C8T6 microcontroller, a dual-channel 2SC0106T2A1-12 gate driver, IRFB4110PbF MOSFETs, and ACS37002 current sensors. The power stage uses $L1 = L2 = 100 \mu\text{H}$ inductors with a saturation current of at least 25 A, a 100 μF transfer film capacitor rated for 200 V, and 1000 μF input/output capacitors with low ESR supplemented by film and ceramic capacitors for high-frequency ripple suppression. This configuration enables operation as a bidirectional PPC compensation stage in both traction and regenerative energy-flow directions.

5. Comparative Analysis with a Bidirectional Full-Power DC-DC Converter

5.1. Experimental Setup

To evaluate the architectural effect of PPC, a prototype bidirectional PPC converter was built and tested. Its results were compared with those of a conventional bidirectional full-power converter implemented on the same component base. This makes it possible to attribute the observed differences primarily to architecture rather than to the superiority of particular components.

The measurements were carried out in steady-state operating conditions. A power supply was connected on one side of the converter and a resistive load on the other. Voltage was measured with both a PicoScope oscilloscope and digital multimeters to cross-check the readings. Current was measured using ACS37002 current sensors, and the corresponding waveforms were recorded by the oscilloscope. Since the goal of the present study was to compare steady-state efficiency, transient processes at startup and under load changes were not analyzed.

For each operating point, the measurement was repeated $n = 10$ times after the converter reached steady-state operation. During each run, input voltage, output voltage, input current, and output current were recorded. The input and output powers were calculated as

$$P_{in} = U_{in}I_{in}, P_{out} = U_{out}I_{out}. \quad (4)$$

Converter losses were determined as

$$P_{loss} = P_{in} - P_{out}. \quad (5)$$

and efficiency was calculated as

$$\eta = \frac{P_{out}}{P_{in}} 100\% . \quad (6)$$

The values presented in Tables 2 and 3 are arithmetic mean values of 10 repeated steady-state measurements. The repeatability of the measurements was evaluated using the standard deviation

$$s = \sqrt{\frac{1}{n-1} \sum_{i=1}^n (P_{loss,i} - \bar{P}_{loss})^2} . \quad (7)$$

For all operating points, the standard deviation of the measured converter losses did not exceed 0.08 W for the PPC configuration and 0.15 W for the full-power configuration. These deviations are considerably smaller than the difference between PPC and full-power converter losses; therefore, the observed loss reduction can be attributed mainly to the converter architecture.

5.2. Traction-Mode Results

When the module is supplied at 24 V, the active PPC cell processes only one third of the full power. As the current increases, its losses rise much more slowly than those of the full-power converter.

Table 2

Comparison of losses and efficiency in traction mode

Current I_{tr} , A	Load power P_{tr} , W	Processed power $P_{proc,tr}$, W	PPC loss $P_{loss,PPC}$, W	Full-power loss $P_{loss,full}$, W	PPC efficiency η_{ppc} , %	Full-power efficiency η_{full} , %
5	120	40	1.73	2.55	98.58	97.92
10	240	80	2.08	4.70	99.14	98.08
15	360	120	2.56	7.95	99.29	97.84
20	480	160	3.14	12.30	99.35	97.50
22	528	176	3.42	14.35	99.36	97.35

Note: Values are arithmetic mean values of $n = 10$ repeated steady-state measurements

The relative reduction in losses was calculated as

$$\Delta P_{loss} = \frac{P_{loss,full} - P_{loss,PPC}}{P_{loss,full}} 100\% . \quad (8)$$

At the maximum traction current of 22 A, this gives a loss reduction of 76.2%. This result is consistent with the analytical estimate that only 33.3% of the total traction power is processed by the active PPC stage.

5.3. Regenerative-Mode Results

In regenerative operation, energy is transferred from the 16 V module to the 36 V bus. Under these conditions, the PPC converter processes 55.6% of the total power, so the gain in losses is smaller than in traction mode.

Table 3

Comparison of losses and efficiency in regenerative mode

Current I_{reg} , A	Returned power P_{reg} , W	Processed power $P_{proc,reg}$, W	PPC loss $P_{loss,PPC}$, W	Full-power loss $P_{loss,full}$, W	PPC efficiency η_{ppc} , %	Full-power efficiency η_{full} , %
2	32	17.78	1.64	1.79	94.88	94.41
4	64	35.56	1.83	2.25	97.14	96.48
6	96	53.33	2.07	2.89	97.84	96.99
8	128	71.11	2.38	3.71	98.14	97.10
10	160	88.89	2.74	4.70	98.29	97.06

Note: Values are arithmetic mean values of $n = 10$ repeated steady-state measurements

At the maximum regenerative current of 10 A, the relative reduction in losses is 41.7%. This reduction is smaller than in traction mode because the processed-power fraction increases from 33.3% to 55.6%. Therefore, the experimental results confirm the analytical expectation that the PPC advantage decreases as the voltage mismatch between the module and the common DC bus increases.

5.4. Discussion

The comparison of the two architectures shows a pronounced directional asymmetry in the PPC advantage. In the 36 V to 24 V traction case, the active cell processes only one third of the total power, and the reduction in losses is maximal. In the 16 V to 36 V regenerative case, the processed-power fraction rises to 55.6%, so the architectural advantage is smaller.

The obtained results are in agreement with earlier PPC studies, which reported that the main advantage of partial-power conversion is achieved when the voltage difference between the source and the load is relatively small. Previous works on photovoltaic systems, battery interfaces, DC microgrids, and charging applications showed that reducing the processed-power fraction can improve converter efficiency and reduce thermal stress. The present study confirms the same general tendency in a mobile robotic power system. However, unlike most previously reported applications, the considered system combines a low-voltage 36 V common DC bus, bidirectional module operation, and regenerative energy return.

Compared with studies focused on stationary battery storage or charging systems, the robotic application imposes additional constraints. The power converter must be compact, thermally efficient, capable of bidirectional operation, and compatible with distributed modular architecture. The experimental comparison with a full-power converter implemented on the same component base is therefore important because it separates the architectural effect of PPC from possible differences in semiconductor devices, magnetic components, or control hardware.

The loss reduction obtained in traction mode is more pronounced than in regenerative mode. This agrees with the PPC principle because the 24 V traction operating point is closer to the 36 V bus than the 16 V regenerative operating point. Therefore, the results support the conclusion that PPC should be applied selectively in robotic modules whose voltage range remains close to the common-bus voltage.

Physically, this behaviour follows directly from the dependence of PPC on the proximity of the voltage levels at the bus and the module terminals. The smaller the voltage mismatch, the smaller the share of power that has to pass through the active cell, and the lower the absolute losses. PPC is therefore especially promising for modules that operate near the nominal bus voltage and for robotic systems in which reduced thermal stress and reduced cooling requirements are important at the system level.

At the same time, the present experiments were limited to steady-state conditions and to a resistive load. A complete assessment of the concept in a real robot should additionally include transient behaviour, interaction with motor drives and energy buffers, and coordination with the supervisory power-management strategy.

Although the proposed converter architecture was evaluated in the context of a mobile wheeled robot, its application is not limited to robotic systems. The same approach can be used in other battery-powered or multi-source mobile platforms that include several subsystems with different voltage and power requirements. Examples include radio-engineering equipment, distributed computing or embedded processing units, and other modular electronic complexes composed of multiple functional components. In such systems, partial-power conversion can improve overall power-distribution efficiency, reduce thermal stress in the conversion stage, and simplify integration of subsystems connected to a common DC bus. Therefore, the proposed architecture may be considered as a promising solution not only for mobile robotics, but also for a wider class of compact autonomous electrical and electronic platforms.

6. Conclusions

This paper examined the use of a bidirectional partial-power converter in the power supply system of a mobile modular robot with a 36 V common DC bus. The main original contribution of the study is

the experimentally validated comparison of partial-power and full-power bidirectional conversion for a representative low-voltage robotic module operating in both traction and regenerative modes.

The analytical estimation showed that the active PPC stage processes 176 W out of 528 W in traction mode and 88.9 W out of 160 W in regenerative mode. This corresponds to processed-power fractions of 33.3% and 55.6%, respectively. The experimental comparison with a full-power bidirectional converter built on the same component base confirmed that the PPC architecture reduces losses from 14.35 W to 3.42 W in traction mode and from 4.70 W to 2.74 W in regenerative mode.

The results confirm that the PPC advantage is directionally asymmetric and depends strongly on the voltage mismatch between the module and the common DC bus. The largest benefit was obtained in traction mode, where the module voltage is closer to the bus voltage. From a practical perspective, the proposed approach can reduce thermal stress on power electronics, lower cooling requirements, and improve the overall efficiency of modular robotic platforms.

The present study was limited to steady-state operation and resistive-load testing. Future work should include dynamic load profiles, interaction with motor drives, regenerative energy buffering, and coordinated control of several energy-active modules connected to the same DC bus.

Author contributions

Rodions Saltanovs contributed to the conceptualisation of the study, analytical estimation of the processed-power fraction, interpretation of the experimental results, and preparation of the manuscript. Alexey Shevchenko contributed to the converter implementation, experimental setup, measurements, and technical validation of the proposed architecture. Both authors reviewed and approved the final version of the manuscript.

Acknowledgment

This work was supported by European funding through Project No. 2.2.1.3.i.0/2/24/A/CFLA/001, "Development of a Multifunctional Modular Ground Robot," and Project No. 5.1.1.2.i.0/2/24/A/CFLA/002, "Research and Development of a Smart Drone Detector."

References

- [1] Farooq M.U., Eizad A., Bae H.-K. Power solutions for autonomous mobile robots: A survey. *Robotics and Autonomous Systems*, vol. 159, 2023, 104285. DOI: 10.1016/j.robot.2022.104285
- [2] McNulty D., Hennessy A., Li M., Armstrong E., Ryan K.M. A review of Li-ion batteries for autonomous mobile robots: Perspectives and outlook for the future. *Journal of Power Sources*, vol. 545, 2022, 231943. DOI: 10.1016/j.jpowsour.2022.231943
- [3] Agamy M.S., Harfman-Todorovic M., Elasser A., Chi S., Steigerwald R.L., Sabate J.A., McCann A.J., Zhang L., Mueller F.J. An efficient partial power processing DC/DC converter for distributed PV architectures. *IEEE Transactions on Power Electronics*, vol. 29, no. 2, 2014, pp. 674-686. DOI: 10.1109/TPEL.2013.2255315
- [4] Zientarski J.R.R., Pinheiro J.R., Martins M.L.S., Hey H.L. Understanding the partial power processing concept: A case-study of buck-boost dc/dc series regulator. In: *Proceedings of 2015 IEEE 13th Brazilian Power Electronics Conference and 1st Southern Power Electronics Conference (COBEP/SPEC)*, 2015, pp. 1-6. DOI: 10.1109/COBEP.2015.7420092
- [5] Zapata J.W., Kouro S., Carrasco G., Renaudineau H., Meynard T.A. Analysis of partial power DC-DC converters for two-stage photovoltaic systems. *IEEE Journal of Emerging and Selected Topics in Power Electronics*, vol. 7, no. 1, 2019, pp. 591-603. DOI: 10.1109/JESTPE.2018.2842638
- [6] Zientarski J.R.R., Martins M.L.S., Pinheiro J.R., Hey H.L. Series-connected partial-power converters applied to PV systems: A design approach based on step-up/down voltage regulation range. *IEEE Transactions on Power Electronics*, vol. 33, no. 9, 2018, pp. 7622-7633. DOI: 10.1109/TPEL.2017.2765928
- [7] Zientarski J.R.R., Martins M.L.S., Pinheiro J.R., Hey H.L. Evaluation of power processing in series-connected partial-power converters. *IEEE Journal of Emerging and Selected Topics in Power Electronics*, vol. 7, no. 1, 2019, pp. 343-352. DOI: 10.1109/JESTPE.2018.2869370

- [8] Anzola J., Aizpuru I., Romero A.A., Loiti A.A., Lopez-Erauskin R., Artal-Sevil J.S., Bernal C. Review of architectures based on partial power processing for DC-DC applications. *IEEE Access*, vol. 8, 2020, pp. 103405-103418. DOI: 10.1109/ACCESS.2020.2999062
- [9] Li C., Cobos J.A. Classification of differential power processing architectures based on VA area modeling. *IEEE Journal of Emerging and Selected Topics in Power Electronics*, vol. 10, no. 6, 2022, pp. 7849-7866. DOI: 10.1109/JESTPE.2021.3093654
- [10] dos Santos N.G.F., Zientarski J.R.R., Martins M.L.S. A review of series-connected partial power converters for DC-DC applications. *IEEE Journal of Emerging and Selected Topics in Power Electronics*, vol. 10, no. 6, 2022, pp. 7825-7838. DOI: 10.1109/JESTPE.2021.3082869
- [11] de Andrade J.M., Coelho R.F., Lazzarin T.B. Partial power processing and efficiency analysis of dc-dc differential converters. *Energies*, vol. 15, no. 3, 2022, 1159. DOI: 10.3390/en15031159
- [12] Mira M.C., Zhang Z., Andersen M.A.E. Analysis and comparison of dc/dc topologies in partial power processing configuration for energy storage systems. In: *Proceedings of 2018 International Power Electronics Conference (IPEC-Niigata 2018 - ECCE Asia)*, 2018, pp. 1351-1357. DOI: 10.23919/IPEC.2018.8507937
- [13] Gsous O., Rizk R., Barbon A., Georgious R. Review of DC-DC partial power converter configurations and topologies. *Energies*, vol. 17, no. 6, 2024, 1496. DOI: 10.3390/en17061496
- [14] Rojas J., Renaudineau H., Kouro S., Rivera S. Partial power DC-DC converter for electric vehicle fast charging stations. In: *Proceedings of IECON 2017 - 43rd Annual Conference of the IEEE Industrial Electronics Society*, 2017, pp. 5274-5279. DOI: 10.1109/IECON.2017.8216913
- [15] Iyer V.M., Gulur S., Bhattacharya S., Ramabhadran R. A partial power converter interface for battery energy storage integration with a DC microgrid. In: *Proceedings of 2019 IEEE Energy Conversion Congress and Exposition (ECCE)*, 2019, pp. 5783-5790. DOI: 10.1109/ECCE.2019.8912590
- [16] Hassanpour N., Chub A., Blinov A., Vinnikov D. Comparison of full power and partial power buck-boost DC-DC converters for residential battery energy storage applications. In: *Proceedings of 2022 IEEE 16th International Conference on Compatibility, Power Electronics, and Power Engineering (CPE-POWERENG)*, 2022, pp. 1-6. DOI: 10.1109/CPE-POWERENG54966.2022.9880862
- [17] Granello P., Soeiro T.B., van der Blij N.H., Bauer P. Revisiting the partial power processing concept: Case study of a 5-kW 99.11% efficient flyback converter-based battery charger. *IEEE Transactions on Transportation Electrification*, vol. 8, no. 4, 2022, pp. 4372-4383. DOI: 10.1109/TTE.2022.3170286